CONCLUSIONS

Sustained Loading

The strain values in the concrete slab, the reinforcing bars, and the steel beam as well as the downward deflection of the unit were influenced by changes in temperature. The strain values in the concrete slab did not asymptotically approach a maximum. On the other hand, strains (hence stress) in the steel beam and the reinforcing bars appeared to have leveled off to constant values. The neutral axis location also appeared to be stationary and the vertical deflection appeared to have stabilized. As expected, the major portion of the creep deformation occurred during the first 90 days of testing. At the end of 1 year of sustained loading, it appears that although creep deformation continues, the rate of increase of creep is minimal.

Repeated Loading

The results show that the load-displacement curve changed little between the first and last cycles of testing. Insignificant slip was recorded between the concrete slab and steel beams during the static cycles. It is concluded that the strength and stiffness characteristics of the bridge unit are not detrimentally affected by repeated loading for which the unit was designed.

Operating Loading

Results of the operating loading test show that the test unit is able to sustain this loading without permanent set. The behavior of the unit was elastic during the test.

The unit has been placed outside for 2 additional years of sustained loading observation. At the end of that period, the unit will be loaded to flexural failure and the slab will be studied for transverse bending strength.

ACKNOWLEDGMENTS

This paper was developed from a research project sponsored by the Oklahoma Department of Transportation. The authors wish to thank Tim Borg, Jim Schmidt, and Dwight Hixon of the ODOT Research and Development Division and Veldo Goins of the ODOT Bridge Division for their helpful suggestions and assistance.

REFERENCE

1. D.E. Branson. Deformation of Concrete Structures. McGraw Hill, New York, 1977.

Publication of this paper sponsored by Committee on Steel Bridges.

Temperature Problem in a Prestressed Box-Girder Bridge

P. C. HOFFMAN, R. M. McCLURE, and H. H. WEST

ABSTRACT

The temperature effects on an experimental, prestressed concrete, segmental, box-girder bridge were evaluated. Field measurements, including vertical deflections and thermocouple readings for temperature, were collected over a 1-year period under various weather conditions. Critical ambient temperature conditions were gleaned from field observations. With the field observations (surface temperatures) as input, three-, two-, and one-dimensional heat-flow analyses were conducted. The three-dimensional heat-flow analysis was a statistical comparison of temperature readings at various longitudinal locations in the experimental bridge. The two-dimensional analysis involved the collection of hourly temperature readings from 24 thermocouples at the midspan of the test bridge for 18 diurnal cycles within a 1-year period. In addition an alternating-direction implicit finite difference analysis was performed, and the results compared well with the field observations. Finally, a one-dimensional approach was formulated with the application of an initial-value method. This was found to be in agreement with the alternating-direction implicit finite difference model and the collected field data.

In the past, the thermal environment was ignored in the design process except for accounting for the longitudinal movement that could occur and the influence such movement could have on joint integrity. However, relatively recent incidents of bridge distress, including the Newmarket Viaduct in New Zealand (1), the fourth Danube Bridge in Vienna, and the development of a crack 56 ft (17 m) long and 0.20-0.24 in. (5-6 mm) wide in the web of the Jagst Bridge in Untergreisheim (2) have prodded the profession to address the complete structural response to the thermal environment.

A field study was conducted to determine the complexity and magnitude of the temperature problem

in a segmental box girder (3). Then an analytical study was performed to evaluate the severity of the temperature problem with regard to design (4). The significant findings are summarized here.

LOCATION, CONFIGURATION, AND INSTRUMENTATION OF TEST BRIDGE

Field observations were recorded for a segmental, prestressed, box-girder bridge located at the Pennsylvania Transportation Research Facilities, which are adjacent to The Pennsylvania State University's main campus (Figure 1). The test bridge was composed of two curved and superelevated, prestressed box girders, each composed of 17 segments. The complete bridge layout, segment and joint numbers, and cross-sectional dimensions are shown in Figure 2.

FIGURE 1 The Pennsylvania Transportation Research Facilities.

The topography of the site provided an environment that was more severe thermally than the environment to which many bridges are subjected. The terrain at the research facilities consists of gently rolling hills and is completely void of large obstacles. Such topography allows maximum solar radiation to be incident on the bridge surfaces, and such openness maximizes any wind-induced convection. In addition, because the bridge configuration involved a large superelevation and a north-south alignment, the western web exterior surface was subjected to a relatively extreme level of radiation. Normally such radiation on web surfaces would not occur because of the shading provided by the cantilevered flanges.

The temperature measurements were recorded on an Esterline Angus model E1124E multipoint recorder. The field observations of temperature variation proceeded in two stages. The initial portion of the thermal study was concerned with the possibility of a longitudinal temperature variation. This study compared 10 thermocouple (copper versus constantan)

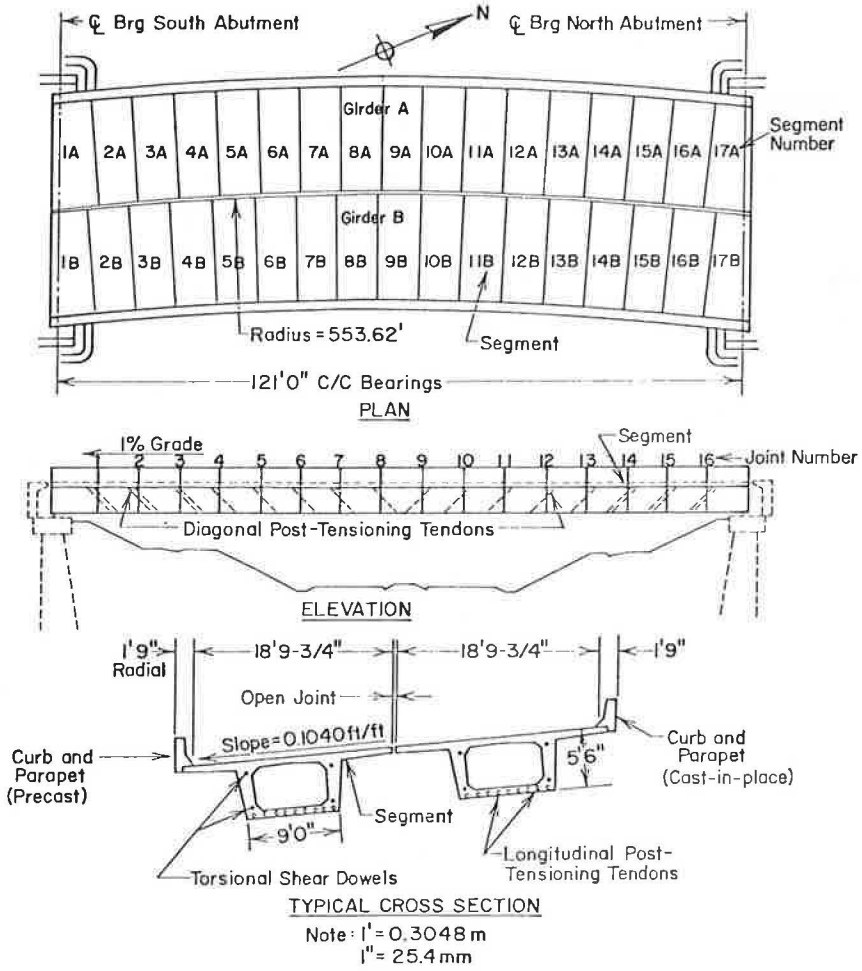

FIGURE 2 Layout and configuration of test bridge.

readings at hourly intervals for three different diurnal cycles between Segments 2A and 5A, and Segments 2A and 9A (Figure 3). When the longitudinal temperature study was concluded, all 24 thermocouples were located at Segment 9A for the transverse temperature study (Figure 4).

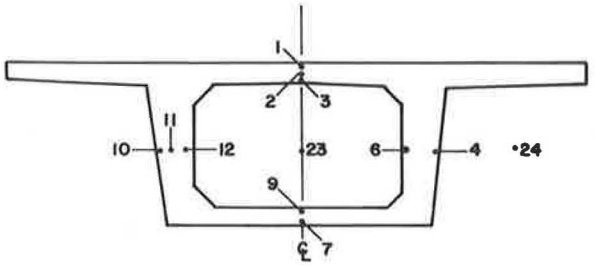

FIGURE 3 Thermocouple locations—longitudinal study.

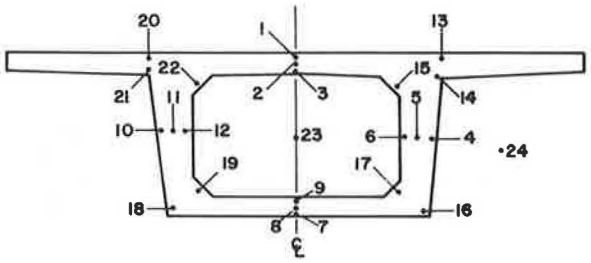

FIGURE 4 Thermocouple locations—transverse study.

The vertical movement of the structure was measured by dial gauges located at both ends and at the midspan of Girder A (Figure 5). The dials had a least count of 0.0001 in. (0.0254 mm). The dials were initially set at the beginning of the readings for the day and left untouched until the termination of the readings at the end of the day. The result of these vertical readings was a set of relative movements from the initial dial readings. Subsequently, the temperature distributions (24 thermocouple readings) were scanned for the set of readings that came closest to a uniform temperature distribution. Then the vertical dial gauge readings were rereferenced to the time of the approximate uniform temperature distribution. The result was the observation of vertical deflections with respect to the equilibrium position under dead load and the prestressing force.

In addition to the data collection at the test site, environmental information was obtained from two other sources. The first source was the Meteorology Observatory at The Pennsylvania State University, which is located approximately 5 miles southeast of the bridge site. The monthly weather summary obtained from the observatory gave the recorded high and low temperatures, the average wind velocity, the sky conditions, and the solar radiation for each day of the month. The second source of meteorological information was the University Park Airport, which is situated approximately 1 mile south of the bridge.

FIELD OBSERVATIONS

The thermal study was initially concerned with the possibility that a significant temperature variation existed in the longitudinal direction of the bridge. To evaluate such a possible variation, temperature readings were taken at Segment 2A and Segment 5A on June 30, 1978, and at Segment 2A and Segment 9A on July 11, 1978, and August 22, 1978, to compare observations for similar thermocouple locations (Figure 3). The ordered pairs of readings were then analyzed both graphically and statistically. From the longitudinal study it was concluded that the heat-flow problem from a practical viewpoint was not three dimensional. Therefore, the complexity of the general heat-flow problem required a two-dimensional study.

In the absence of a longitudinal temperature variation, the vertical deflection measurements can be converted to curvature. Because each transverse section was found to be subjected to the same temperature distribution at any point in time, each transverse section must physically respond in the same manner. In other words, for identical temperature distributions, the induced curvatures must be identical. Therefore, the curvature (M/EI diagram) must be constant. This fact, in turn, means that if the midspan deflection is known, the curvature can be readily determined by appropriate application of the moment area theorems. First, the division of the midspan deflection by a quarter of the bridge span is the angle change between the midspan and the endpoints. Second, the division of the angle change by half of the bridge span equals the curvature at each section. Hence, the vertical deflection measurements in conjunction with the internal thermo-

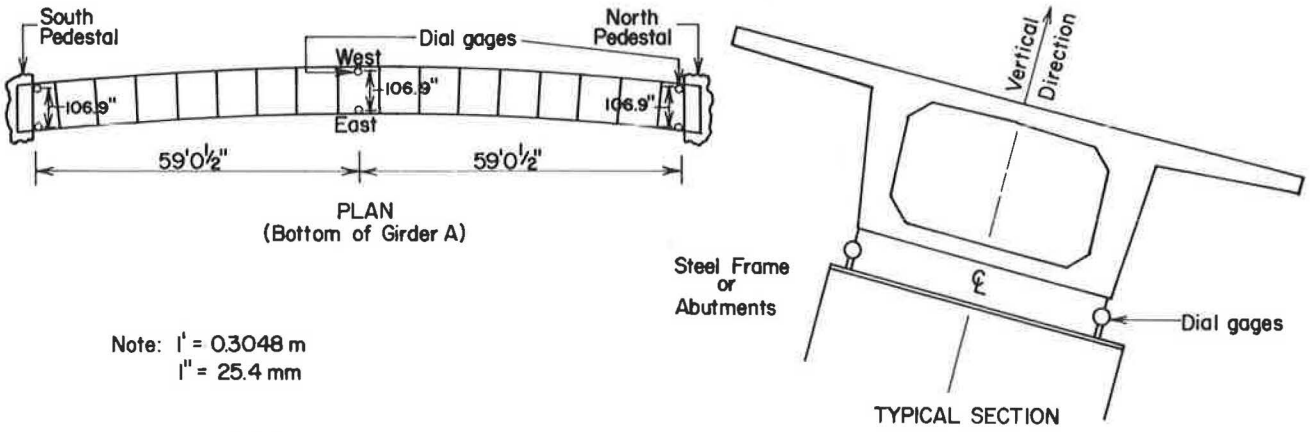

FIGURE 5 Locations of dial gauges.

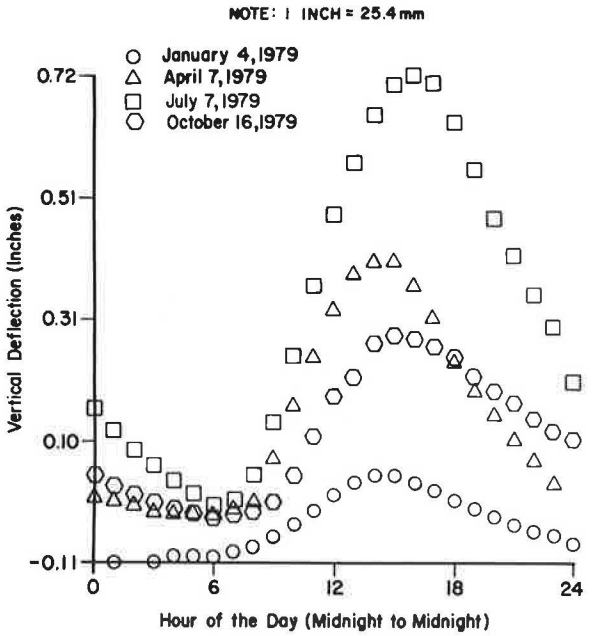

FIGURE 6 Vertical deflections using uniform temperature distribution as reference.

couple readings provided excellent supporting data for the analytic studies.

A graphic display of the seasonal observations of deflections immediately indicated that the extremes occur in winter and summer (Figure 6). The deflections when multiplied by $8/L^2$ (L = span length) are the observed curvatures. The magnitude of the deflections was found to exceed substantially that of the deflections due to live loading (5). Consequently, an effort was undertaken to identify and quantify the inputs that caused the vertical deflections.

The first area of investigation was the effects of ambient air temperature and solar radiation. These thermal inputs could be reasonably measured. With data from the Meteorological Observatory and field readings, comparisons of thermocouple readings, solar radiation, vertical deflections, and ambient air temperature were analyzed for each set of diurnal observations (a total of 18 diurnal cycles). For illustrative purposes, the normalized values of Thermocouple 1, ambient air temperature (Thermocouple 24), solar radiation, and vertical deflection versus time for July 7, 1979, are shown in Figure 7. This figure indicates a relatively large temperature variation for Thermocouple 1 in comparison with the ambient air temperature. The peak values for Thermocouple 1 and for vertical deflection occurred during the same hour, which was 4 hours after the maximum hourly solar radiation. A complete statistical analysis focused on ambient air temperature and solar radiation.

The investigation concluded that exterior surfaces not subjected to direct solar radiation could reasonably be expected to maintain a surface temperature equivalent to the ambient air temperature. For surfaces exposed to direct solar radiation, the temperature was modeled as the sum of the ambient air temperature, a coefficient times the cumulative solar radiation for the previous 4 hours, and a coefficient times the cumulative solar radiation. The coefficient of determination (R^2) indicated a high degree of interrelationship. However, because the data base was limited, a definitive statement about the values of each of the coefficients could not be formulated. The statistical analysis did verify the fact that ambient air temperature and solar radiation were the two major inputs to the thermal problem. In other words, heat convection and reradiation were present but were not observed to cause any significant problems.

TWO-DIMENSIONAL ANALYTICAL STUDY

The findings from the field observations indicated that the temperature problem was, in its most complex form, a two-dimensional problem. From a practical viewpoint, temperature-induced bridge movements were defined as the critical design concerns. To evaluate the magnitudes of deflection in both the horizontal and vertical directions, a two-part analytical scheme was developed. The first, numerical

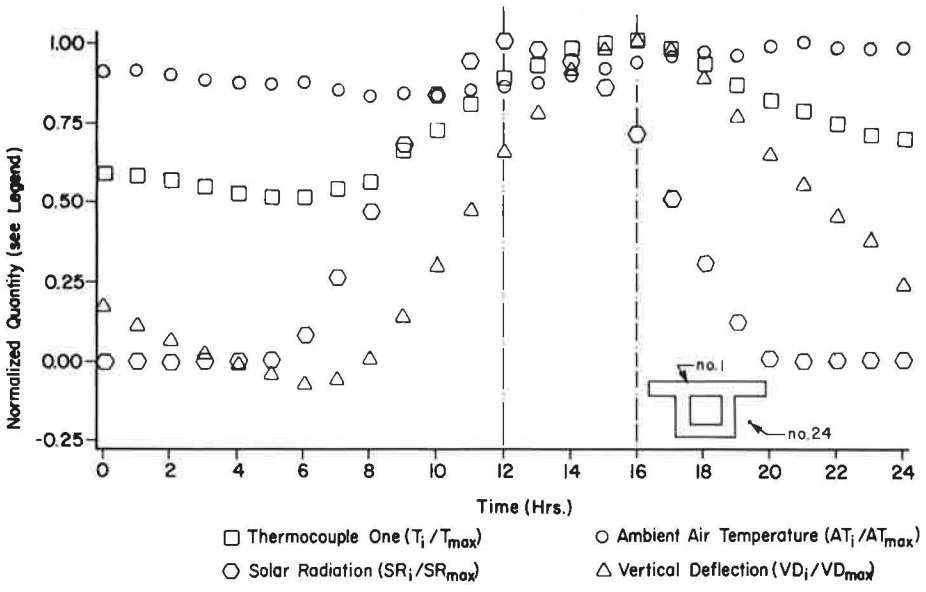

FIGURE 7 Normalized curves, July 7, 1979.

part was a two-dimensional analysis of the transient heat-flow process to determine temperature distributions. The second part used the temperature distributions as input for the computations of curvatures about the x and y axes.

The determination of the temperature distribution of the transient heat-flow problem for an isotropic material required a numerical solution to the parabolic differential equation

$$\partial^2 T/\partial x^2 + \partial^2 T/\partial y^2 = 1/\alpha\, \partial T/\partial t \quad (1)$$

where

T = temperature at point (x,y),
x,y = coordinate axes,
t = time, and
α = thermal diffusivity.

The alternating-direction implicit finite difference method was used as the numerical technique. The observed surface temperatures (field study) were used as the boundary conditions, and the observed internal temperature readings were used to validate the numerical technique.

The computation of curvatures consisted of a double summation (6) as follows:

$$\phi_y = \alpha/I_x \sum_{i=1}^{n} \sum_{j=1}^{m} t(x_i y_j) \cdot y_j \cdot \Delta x \Delta y \quad (2)$$

$$\phi_x = \alpha/I_y \sum_{i=1}^{n} \sum_{j=1}^{m} t(x_i y_j) \cdot x_i \cdot \Delta x \Delta y \quad (3)$$

where

ϕ_y = curvature due to bending about x axis,
ϕ_x = curvature due to bending about y axis,
α = coefficient of thermal expansion,
I_x = second moment of area about the x axis,
I_y = second moment of area about the y axis, and
t(x,y) = temperature variation as a function of x and y.

Such formulation of the temperature effect is valid because the temperature does not vary longitudinally. Therefore, the curvature would be invariant, which leads to the conclusion that bending deformations must also be constant. With constant curvatures corresponding to bending about each of the two principal axes, twisting is nonexistent, and the thermal response can be viewed as the superposition of these two curvatures.

Several observed surface temperature cycles were applied to the numerical model, and the resulting curvatures were computed (Figure 8). The conclusion was that the bending action about the major axis for box sections with overhanging flanges was very small. The small rise in the major-axis curvature plot (from 20 to 23) was probably due to the sudden jump in the exterior surface temperature of the western web, resulting from the setting sun (Figure 9). However, the interior temperatures showed little change with the sudden rise in surface temperature. Therefore, it was concluded that the existence of major-axis bending was negligible. Consequently, a one-dimensional analysis was feasible for the determination of significant bridge movement.

ONE-DIMENSIONAL ANALYTICAL STUDY

The one-dimensional heat-flow analysis emphasized evaluating structural movement under the thermal environment. In addition, the residual stresses (the equilibrating stresses that remain after the development of curvature and expansion) due to the nonlinear temperature distributions were computed. The analysis consisted of applying the initial-value method to determine the temperature variation with depth (4). Then a single summation simplification of Equation 3 was used to find curvatures.

The initial-value method is a numerical method that discretizes the one-dimensional heat conduction equation

$$\partial^2 T/\partial y^2 = 1/\alpha\, \partial T/\partial/t \quad (4)$$

and is applied to a nodal pattern (Figure 10). In the field study, the surface temperatures, which were taken as the known boundary conditions for Equation 4, were measured on the hour. Also, the rate of change of temperature at the top surface (Node 1) was linearly approximated as

$$(\partial T/\partial t)_1 \approx (T_1^{k+1} - T_1^k)/60 \quad (5)$$

where T_1^k is the observed surface temperature at Node 1 at the kth hour.

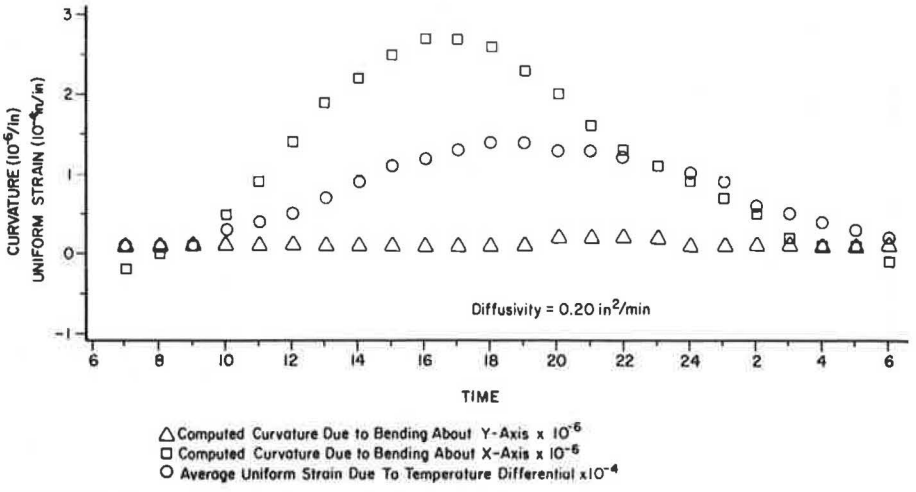

FIGURE 8 Computed numerical results for July 7, 1979.

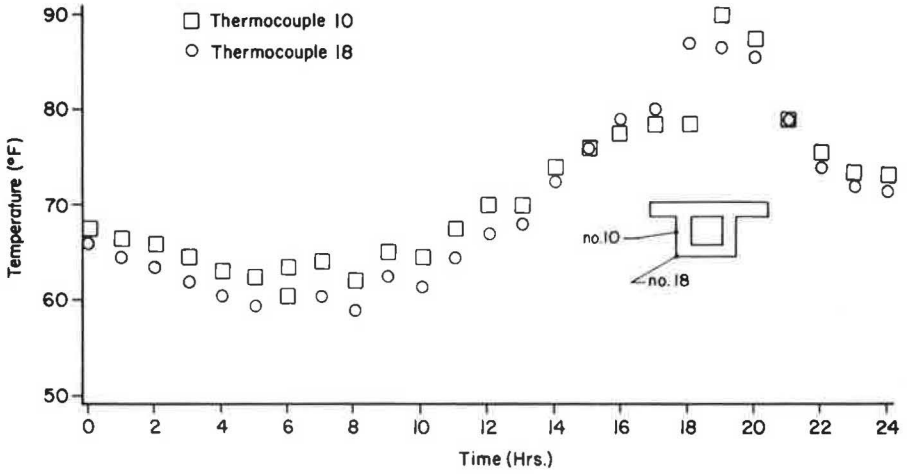

FIGURE 9 Exterior web temperatures, July 7, 1979.

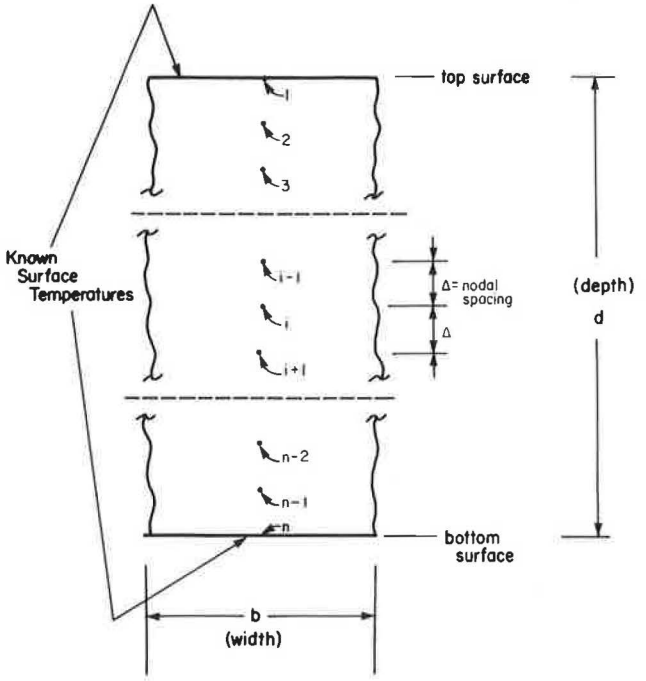

FIGURE 10 Nodal formulation.

If the first partial derivative of temperature with respect to depth ($\partial T/\partial y$) were known at the top surface, then a simple numerical integration from the first node (top surface) to the second node could be conducted. Consequently, the procedure would terminate at the nth node (bottom surface), with the results being the nodal temperature distribution. However, the correct value for the first partial derivative of temperature with respect to depth is an unknown. If an assumed value for the first partial derivative is used in the integration, then the particular temperature at the nth node $(T_n)_p$ would in all likelihood differ from the observed value. Any error is due solely to the error in the assumed first partial derivative at the top surface. Therefore, a separate homogeneous solution vector could be developed from an assumed first partial derivative with respect to depth (any value other than zero) and a top surface temperature of zero degrees. The second solution vector (nodal temperatures) consists of numerical partial derivatives; that is, the ith element gives the rate of change of temperature at Node i with respect to a change in the first partial derivative with respect to depth at Node 1. Hence, a linear combination of the two numerical solutions for the nth node (bottom surface) can be formulated such that the sum equals the observed temperature:

$$(T_n)_p^{p+1} + C \cdot (T_n)_h^{p+1} = (T_n)_o^{p+1} \tag{6}$$

where

$(T_n)^{p+1}$ = temperature at nth node at time period p + 1,
p = subscript for particular solution,
h = subscript for homogeneous solution, and
o = subscript for observed value.

When the coefficient (C) has been determined from Equation 6, the interior nodal temperatures are readily computed from

$$(T_i)_c^{p+1} = (T_i)_p^{p+1} + C \cdot (T_i)_h^{p+1} \tag{7}$$

where $(T_i)_c^{p+1}$ is the computed temperature at Node i. From the computed nodal temperatures, the curvature can be determined by a simplified version (single summation) of Equation 3.

To apply the one-dimensional analysis, the box section was divided into sections and a heat-flow analysis was performed on each section (Figure 11). The vertical temperature distribution was assumed to

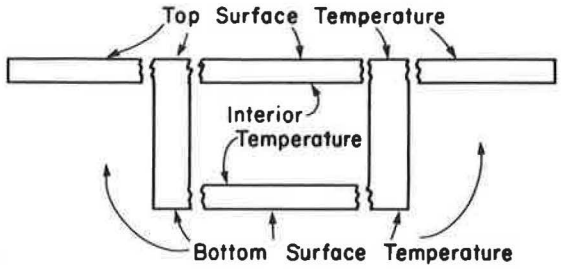

FIGURE 11 Sectional subdivision of box sections for one-dimensional heat-flow analysis.

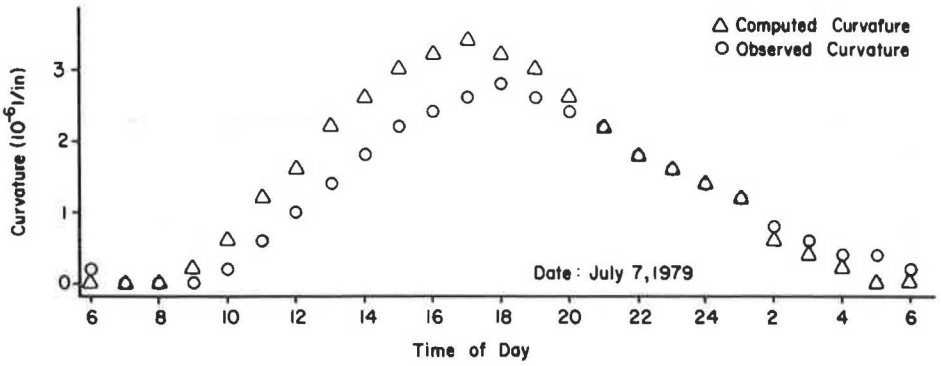

FIGURE 12 Observed curvature versus computed curvature.

be constant across the width of each section: webs, flange, and soffit. This approach has some degree of error because it allows discontinuities at the intersection of the members. However, the error is localized at specific points, and comparisons between the observed values and the numerical values displayed good agreement (Figure 12). It was noted that the computed curvatures disagreed with the observed values by approximately 20 percent. However, the same discrepancy was experienced in static load testing of the bridge (5). Therefore, it was concluded that the end conditions of the bridge developed a rotational restraint of 20 percent fixity. Hence, the one-dimensional approach seemed applicable for the evaluation of deflections.

As a final investigation, the residual stresses in the bridge structure were analyzed. When a bridge is subjected to a nonlinear temperature differential, t(y), the bridge will respond by elongating (due to the incremental change in the mean temperature) and hogging or sagging (due to the difference in temperature). Hence, a uniform strain from the longitudinal change in length ($\epsilon = \Delta L/L$) and a curvature strain ($\phi \cdot y$) develop. These two strains occur at the same time that a thermal strain, $\alpha \cdot t(y)$, would develop if the end conditions were fully restrained. Therefore, the combination of strain developments multiplied by Young's modulus (E) determines the magnitude of the residual stress (f_r):

$$f_r = E[\phi \cdot y + \epsilon - \alpha t(y)] \quad (8)$$

The temperature distribution that caused the maximum curvature development for July 7, 1979, was determined by the initial-value method (Figure 13). Then, by applying Equation 8, the residual stress distribution was computed (Figure 14). The tempera-

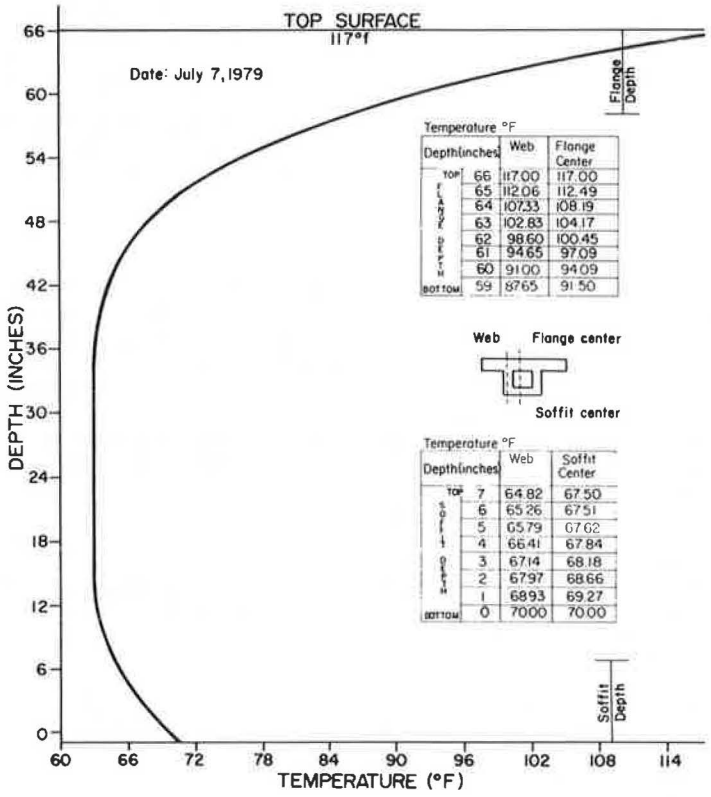

FIGURE 13 Web temperature with depth as computed by the initial-value approach (5:00 p.m.).

the one- and the two-dimensional analyses gave the same magnitude for the residual stress problem, but occurrence in the cross section differed. With the presence of unsymmetrical thermal boundary conditions, therefore, a one-dimensional approach (Figure 11) could be misleading with respect to a residual stress distribution.

Therefore, because of the multitude of possible thermal surface conditions, a simple analytical model is not feasible at this time. However, most design specifications account for the possible combinations of loading extremes by allowing a percentage increase (usually 33 1/3 percent) above the specified working stress limitation. Therefore, it should prove adequate to specify a 600 psi increase in the actual working stress, considering the percentage increase in the allowable working stress. Until more extensive work is performed, such a simplified approach seems prudent.

REFERENCES

1. M.J.N. Priestley. Thermal Gradients in Bridges: Some Design Considerations. New Zealand Engineering, Vol. 27, No. 7, July 1972, pp. 228-233.
2. W.J. Price. Introductory Note, Bridge Temperatures. TRRL Report SR442. Transport and Road Research Laboratory, Crowthorne, Berkshire, England, 1978.
3. P.C. Hoffman, R.M. McClure, and H.H. West. Temperature Studies for an Experimental Segmental Bridge. Research Project 75-3, Report PTI 8010. Pennsylvania Transportation Institute, Pennsylvania State University, University Park, 1980.
4. P.C. Hoffman. Thermal Design Considerations for an Experimental Prestressed Segmental Box Girder. Ph.D. dissertation. Pennsylvania State University, University Park, 1982.
5. R.M. McClure and H.H. West. Field Testing of an Experimental Segmental Bridge. Research Project No. 75-3, Report PTI 8009. Pennsylvania Transportation Institute, Pennsylvania State University, University Park, 1980.
6. M.J.N. Priestley and I.G. Buckle. Ambient Thermal Response of Concrete Bridges. Bulletin 42. Roads Research Unit, National Roads Board, New Zealand, 1979, pp. 26-27.
7. P.C. Hoffman, R.M. McClure, and H.H. West. Temperature: A Service Design Problem. Proc., National Bridge Conference, Pittsburgh, Pa., June 1983.

This study covers only a portion of a major 6-year investigation of an experimental segmental bridge that was conducted at The Pennsylvania Transportation Institute of The Pennsylvania State University. This study was sponsored and funded by the Pennsylvania Department of Transportation and the FHWA. The contents of this paper reflect the views of the authors, who are responsible for the facts and the accuracy of the data. The contents do not necessarily reflect the official views or policies of the sponsors.

Publication of this paper sponsored by Committee on Concrete Bridges.

Seasonal and Diurnal Behavior of Concrete Box-Girder Bridges

K. NAM SHIU

ABSTRACT

Measurements from three instrumented bridges in different parts of the United States were used to assess seasonal and diurnal behavior of concrete box-girder bridges. Effective bridge temperatures were used to evaluate seasonal thermal changes in bridges. Effective bridge temperature is defined as the temperature that governs longitudinal bridge movements. The effective bridge temperatures followed the same seasonal fluctuation as monthly average air temperature at the bridge site. Measured temperature differentials from top to bottom slabs for the three box-girder bridges were between +20°F and -10°F (+11.1°C and -5.6°C) regardless of geographic location. Temperature differentials were calculated by subtracting temperatures of the bottom slab from those of the top slab. Diurnal behavior of one bridge was continuously monitored for 24 hours during each of the four seasons. Longitudinal strains and temperatures were used to evaluate effects of nonlinear temperature gradient on bridge behavior. Internal thermal stresses at the instrumented bridge sections are reported.

Most materials expand with a rise in temperature and contract with a fall in temperature. In the past designers have assumed that structures respond lin-